International Conference on Space Optics—ICSO 2008

Toulouse, France

14–17 October 2008

Edited by Josiane Costeraste, Errico Armandillo, and Nikos Karafolas

A novel optical design for the stereo channel of the imaging system SIMBIOSYS for the BepiColombo ESA mission

Vania Da Deppo

Giampiero Naletto

Gabriele Cremonese

Luciano Calamai

et al.

esa icso proceedings cnes

International Conference on Space Optics — ICSO 2008, edited by Josiane Costeraste, Errico Armandillo, Nikos Karafolas, Proc. of SPIE Vol. 10566, 105661S · © 2008 ESA and CNES
CCC code: 0277-786X/17/$18 · doi: 10.1117/12.2308273

A NOVEL OPTICAL DESIGN FOR THE STEREO CHANNEL OF THE IMAGING SYSTEM SIMBIOSYS FOR THE BEPICOLOMBO ESA MISSION

Vania Da Deppo[(1),(2),(4)], Giampiero Naletto[(1),(2(,(3),(4)], Gabriele Cremonese[(4),(2)], Luciano Calamai[(5)], Stefano Debei[(2),(6)], Enrico Flamini[(7)]

[(1)]CNR-INFM LUXOR, Via Gradenigo 6/B, 35131 Padova, Italy, e-mail: dadeppo@dei.unipd.it
[(2)]CISAS, Via Venezia 15, 35131 Padova, Italy
[(3)]Department of Information Engineering, Via Gradenigo 6/B, 35131 Padova, Italy
[(4)]INAF - Osservatorio Astronomico di Padova, Vicolo dell'Osservatorio 5, 35122 Padova, Italy
[(5)]SELEX-GALILEO, Via A. Einstein 35, 50013 Campi di Bisenzio (FI), Italy
[(6)]Department of Mechanical Engineering, Via Venezia 1, 35131 Padova, Italy
[(7)]ASI – Italian Space Agency, Viale Liegi 26, 00198 Roma, Italy

ABSTRACT

In this paper the design of a novel catadioptric optical solution for the Stereo Channel (STC) of the imaging system SIMBIOSYS for the BepiColombo ESA mission to Mercury is presented.
The main scientific objective is the 3D global mapping of the entire surface of Mercury with a scale factor of 50 m per pixel at periherm in five different spectral bands.
The system consists of two sub-channels looking at ±20° from nadir. They share the detector and all the optical components with the exception of the first element, a rhomboid prism. The field of view of each channel is 5.3° × 4.5° and the scale factor is 23 arcsec/pixel. The system guarantees an aberration balancing over all the field of view and wavelength range with optimal optical performance.
For stray-light suppression, an efficient baffling system able to well decouple the optical paths of the two sub-channels has been designed.

1. INTRODUCTION

Bepicolombo is a cornerstone mission of the European Space Agency (ESA) with the aim of studying in great detail Mercury, the innermost planet of the Solar System.
Mercury is very important from the point of view of testing and constraining the dynamical and compositional theories of planetary system formation.
In fact, being in close proximity to the Sun it has been subjected to a rather peculiar environment, such as large temperature and high diurnal variation, rotational state changed by Sun induced tidal deformation, surface alteration during the cooling phase and chemical surface composition modification by bombardment in early history.
Mercury has been studied only by the Mariner 10 spacecraft (S/C) in 1974-75 [1,2,3], when less than half of the planetary surface has been imaged at low resolution (scale factor of about 1-2 km/px) and its magnetic field has been discovered. Since then, the only other satellite reaching Mercury is the NASA Messenger, that has very recently realized a flyby with the planet; Messenger will be inserted in orbit around Mercury in March 2011.
The BepiColombo payload, especially designed to fully characterize the planet, will consist of two modules: the Mercury Planet Orbiter (MPO), realized in Europe, carrying remote sensing and radio science experiments, and the Mercury Magnetospheric Orbiter (MMO) [4], realized by JAXA in Japan, carrying field and particle science instrumentation. These two complementary packages will allow to map the entire surface of the planet, to study the geological evolution of the body and its inner structure, i.e. the main MPO tasks, and to study the magnetosphere and its relation with the surface, the exosphere and the interplanetary medium, i.e. MMO targets.
To achieve the mission objectives, the orbits of the two modules are rather different: MMO will be put in a highly elliptical polar orbit with periherm and apoherm altitudes of 400 km and 12000 km and 9.2 hours orbital period; MPO will be in a slightly elliptical polar orbit with periherm and apoherm altitudes of 400 km and 1500 km and 2.3 hours orbital period.
The MPO orbital characteristics are mainly determined by the need for the remote sensing instruments to have high spatial resolution not changing too much all over the surface during the one year nominal mission lifetime, and they are extremely challenging due to the thermal constraints on the S/C. For a continuous observation of the planet surface during the mission, the S/C is 3-axis stabilized with the Z-axis, corresponding to payload boresight direction, pointing to nadir.

1.1 SIMBIOSYS

The MPO module is carrying instruments which are devoted to the close range study of Mercury surface, to

the investigation of the planet gravity field, of the inner magnetosphere and of the exosphere. Imaging and spectral analysis are performed in the IR, visible and UV range. These optical observations are complemented by those of gamma-ray, X-ray and neutron spectrometers, which yield additional data about the elemental composition of the surface, and by those of a laser altimeter, BELA [5], dedicated to high accuracy measurements of the surface figure, morphology and topography.

The imaging and spectroscopic capability of the MPO modulus will be exploited by the Spectrometers and Imagers for MPO BepiColombo Integrated Observatory SYStem (SIMBIOSYS), that is an integrated system for imaging and spectroscopic investigation of the Mercury surface. A highly integrated concept is adopted to maximize the scientific return while minimizing resources requirements, primarily mass and power [6].

SIMBIOSYS incorporates capabilities to perform 50-110 m spatial resolution global mapping in both stereo mode and color filters, high spatial resolution imaging (5 m/px scale factor at periherm) in panchromatic and broad-band filters, and imaging spectroscopy in the spectral range 400-2000 nm. This global performance is reached using three channels: STC [7], the STereo imaging Channel; HRIC, the High Resolution Imaging Channel [8]; and VIHI, the Visible and near-Infrared Hyperspectral Imager [9].

2. THE STEREOSCOPIC IMAGING CHANNEL

STC is a double wide angle camera designed to image each portion of the Mercury surface from two different perspectives, providing panchromatic stereo image pairs required for reconstructing the Digital Terrain Model (DTM) of the planet surface. In addition, it has the capability of imaging some portion of the planet in four different spectral bands (see Fig. 1).

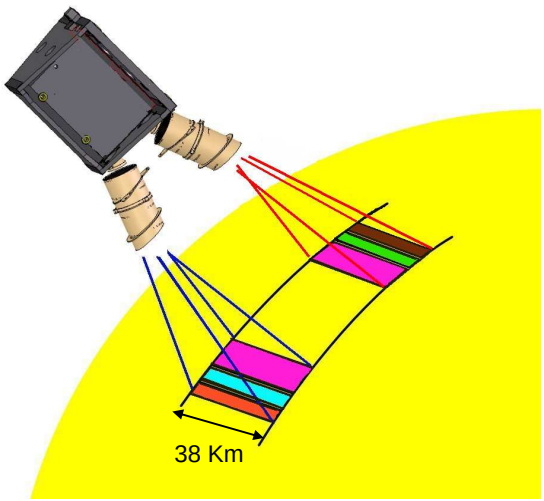

Fig. 1 STC concept.

2.1 STC scientific requirement

The main scientific requirement for the STC is to provide the global panchromatic coverage of the surface and secondly to study selected areas in predefine spectral bands [10]. Both imaging tasks should be accomplished with a mean scale of 110 m/px (minimum of 50 m/pixel at the equator). The spectral bands have been chosen with the aim of studying surface composition and defining the main geological units. The STC stereo channel will allow to analyze the morphology of the tectonic features, the impact craters and the volcanic edifices. The STC will also provide the context for the HRIC investigation.

A stereo imaging system has to satisfy a series of scientific requirements linked not only to common optical performance definition, but also to the additional constraints imposed by photogrammetry.

The overall camera requirements are reported in Tab. 1. The scale factor and the swath at periherm have been defined to be able to map the whole Mercury surface during the mission lifetime. For reaching the required 80 m vertical accuracy in the DTM, a standard satellite stereo imaging solution [11,12] has been chosen, with two panchromatic sub-channels looking at ±20° from nadir. The required optical performance of STC is expressed in terms of the Ensquared Energy (EE) inside one pixel, or alternatively in terms of the Modulation Transfer Function (MTF) at the detector Nyquist frequency.

Tab. 1 STC scientific requirements.

Scale factor	50 m/px at periherm
Swath	38 km at periherm
Stereoscopic properties	±20° stereo angle with respect to nadir both images on the same detector
Vertical accuracy	80 m
EE MTF	> 70% inside 1 pixel > 60% at Nyquist frequency
Wavelength coverage	410-930 nm (5 filters)
Filters	panchromatic (700 ± 100 nm) 420 ± 10 nm 550 ± 10 nm 750 ± 10 nm 920 ± 10 nm

2.2 STC optical design

The design of the camera has been driven not only by the just described scientific requirements but also by the aim of saving mass and power. In this attempt, an optical solution in which the detector and most of the optical elements are shared by the two channels has been studied. The design has been kept as short as possible, compatibly with the need of limiting the

cross-talk between the two channel and to cope with stray-light problems due to the common optics choice.
The desired 50 m/px scale factor at periherm is reached with a 90 mm effective focal length, considering the 10 microns pixel size of the Si_PIN hybrid detector chosen. This kind of detector is particularly useful both in terms of radiation hardness, given the hostile Mercury environment, and for the capability of snapshot image acquisition, which is less demanding in terms of S/C pointing and stability.
The adopted telescope optical solution (see Fig. 2) is a novel design, in which a couple of rhomboid prisms redirects the ±20° wide open beams along directions much closer to the system optical axis. After the two prisms, a modified Schmidt telescope follows, in which a correcting doublet positioned at about half distance between the spherical mirror M1 and its center of curvature replaces the classical Schmidt correcting plate. In this way, the telescope length is reduced by about a factor of two with respect to the classical solution. Finally, a field correcting system has been included just in front of the detector.

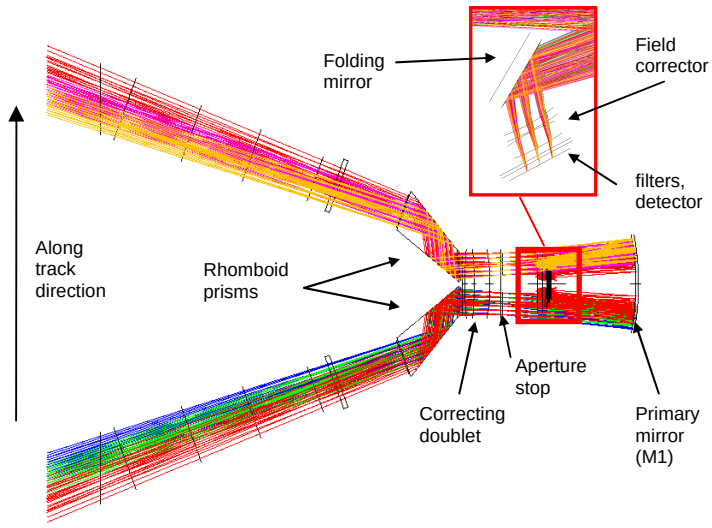

Fig. 2 STC overall optical design layout. The inset shows a different projection of the focal plane region.

The nominal FoV of each sub-channel is 5.3° × 4.5° subdivided in 3 narrow strips, one for each filter, covering three quasi-contiguous areas on Mercury surface (see Fig. 1); the scientific useful FoV is actually slightly smaller, 5.3° × 3.2°, imposed by the filter strip solution choice. At periherm, each panchromatic strip corresponds to an area of about 40×19 km^2, and each colored strip to an area of about 40×3 km^2.
The optical characteristics of the camera are summarized in Tab. 2.

Tab. 2 STC optical characteristics.

Optical concept	Catadrioptic: modified Schmidt telescope plus rhomboid prisms and field corrector
Stereo solution (concept)	2 identical optical channels; Detector and most of the optical elements common to both channels
Focal length (on-axis)	90 mm
Pupil size (diameter)	15 mm
Focal ratio	*f*/6
Mean image scale	23 arcsec/px (111 µrad/px)
FoV (cross track)	5.3°
FoV (along track)	2.4° pancromatic 0.4° color filters
Detector	Si_PIN (format: 2048 × 2048; 10 µm squared pixel). 14 bits dynamic range

Simulation and optimization of the camera design have been done by means of Zemax ray-tracing software.
The design has been chosen to satisfy the desired optical performance for all the filters in the whole FoV of each filter. Being the wavelength range rather extended, the on-axis and lateral chromatic aberrations tend to be the worst offenders in the optimization of the system. Given the high radiation dose to which the optical elements will be exposed to, the choice of the glasses has to be restricted to rad-hard ones, and to simplify the procurement all the lenses are foreseen in fused silica.
The off-axis value of the telescope has been driven by the free back focal length, that has to be sufficient to easily integrate the Focal Plane Assembly, maintaining the required optical performance.
The correcting doublet has an essentially null optical power, and its function is to correct the residual aberrations of the primary mirror. Being the doublet optical power near to zero, the residual chromatic aberration in terms of primary and secondary colors is negligible over the whole 410-930 nm spectral range.
The Aperture Stop (AS) position, placed in the front focal plane of the spherical M1 mirror, just after the correcting doublet, has been chosen to allow a good aberration balancing over all the FoV and to guarantee the telecentricity of the design. In fact, being the filter window placed in the converging light beam near the detector, to avoid wavelength shifts due to non orthogonal incidence of the beam on the filter itself, the camera design has been kept as telecentric as possible.
To cope with the field dependent aberrations (i.e field curvature, lateral color,..) a two-lens field corrector has been designed to be placed in front of the detector (see Fig. 2). In addition the solution chosen for the filter manufacturing, i.e. a single optical element composed

of stripe-butted filters, allows a better control of the chromatic aberration in the single FoV of each filter.
The rhomboid prism couple, as already mentioned, redirects the ±20° inclination with respect to nadir of the incoming beam to a much smaller ±3.75° one, allowing a much simpler system optical design. These prisms can be made of either BK7G18 or Fused Silica radhard glasses; the reflection of the beam inside the prism takes advantage of the total internal reflection at the glass-air interface.

2.3 Stray-light control

From the point of view of stray-light control the system is very challenging being most of the optical elements common to both sub-cannels. The useful optical beam of the two sub channel has been kept as far apart as possible within the allocated volume, including the choice of using an inclination as high as possible on the beam exiting the prism and directed toward the M1 mirror. In this way, the internal edges of each sub-channel radiation beam are well separated, about 4 mm on the detector active surface.
To prevent cross-talk between the two paths of the two sub-channels, a suitable internal and external baffling system, including baffles at the entrance and exit of the prism and in the middle of all the optical elements, has been designed. A good means to control the stray-light is given by the position chosen for the AS, just after the first correcting doublet: the majority of the stray-light coming from the preceding optical elements, is blocked at this point.
Simulations done with Opticad software show that no direct cross-talk between the two subchannels is present. Moreover, it has been verified that the vignetting function is sufficiently steep to maintain totally decoupled the two optical paths even if the closest distance between the respective images on the common detector is of only 4 mm.
Also the in-field stray-light has to be taken into account and assessed. The main contribution to the in-field stray-light is given by the ghost images coming from the filter and the detector surface beam reflections. The relatively high inclination (~23°) of the beam with respect to the filter and detector normals keeps the ghosts far from the primary useful image, but, owing to the filter "spatial" extension small portions of the ghosts fall anyway over detector useful areas. A correct choice of filter position and size in the filter strip stack helps to reduce the phenomenon.
A preliminary analysis of the ghost image intensities has been done on the basis of the expected reflective properties of filters and detector, and of the spectral distribution of the incoming flux. The results show that the stray-light level coming from the ghost images can be controlled if the panchromatic filter is positioned at the center of the filter stack and if an appropriate filter masking is foreseen. One, or two, masks on the filter strip assembly can stop the ghost beam coming from each filter strip and prevent it to be reflected on the adjacent one. In that case the ratio between the ghost image intensity and the useful image one can be less than 10^{-3}; otherwise, if the mask is not realized, in the worst case ghost intensity ratios as high as 10^{-2} can arise.
A preliminary stray-light analysis also for light sources outside the STC FoV has been performed, based on the expected properties of the coating for the internal and external baffle vanes and the optical surface scattering and reflectivity properties.
The primary source of stray-light outside FoV is the Mercury surface itself: in the worst case, at periherm, the surface of Mercury covers a FoV of about 120° in diameter. This stray-light contribution is mainly blocked by the suitably sized external baffle and the AS; its level is reduced to a value smaller than the noise appreciable by the detector.
In fact, the results of the simulation of the system show that a point source outside the FoV, for directions which are inclined more than 30° with respect to the sub-channel boresight direction, gives a relative stray-light signal smaller than $6\ 10^{-9}$. For sources in the range between the edges of the FoV and the 30° inclination, the relative spurious signal is lower than $5\ 10^{-5}$.
Integrating over all the surface of Mercury, the global stray-light value on one pixel, compare to the useful signal measured for one pixel extended element source on the Mercury surface, is about 10^{-4}. This value is low if compared to the noise expected from the other sources (i.e. electronics noise, photonic noise,..).

2.4 STC performance

The performance of the camera has been calculated for all the filters in the whole FoV; spot diagrams and EE have been considered.
The spot diagrams and the relative EE for the panchromatic filter are shown respectively in Fig. 3 and Fig. 4. It can be seen that the spots are well within the overlaid box having the 10 µm square pixel size of the foreseen detector; a small lateral color residual is present in one corner of the field, but it has been verified to be less than 1/3rd of a pixel, that is completely tolerable.
The mean diffraction EE has been calculated over all the FoV of each filter and over the wavelength band of the filter itself. The EE including diffraction effects is of the order of 80% all over the FoV of each filter ($5.3° \times 2.4°$ panchromatic; $5.3° \times 0.4°$ color filter); it is a few percent smaller only for the filter centered at 420 nm, where some chromatic focal shift is present.
Also the MTF of the optical system has been derived for all the filters in the whole FoV. The mean MTF, at the Nyquist frequency of 50 cycle/mm, is of the order of 60-70%. As an example, the mean MTF for the panchromatic filter is shown in Fig. 5.

Considering that a reasonable value for the detector MTF is 50-60%, the global MTF of the system, including detector sampling, is of the order of 30 %.

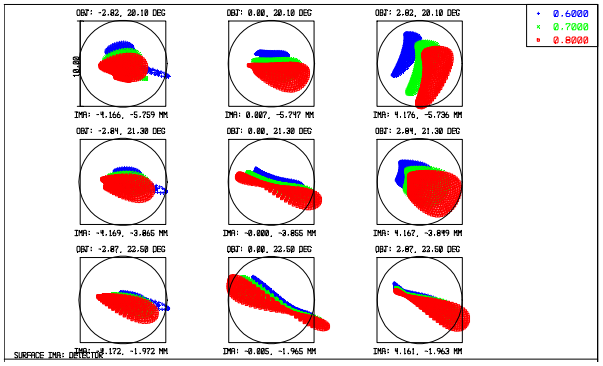

Fig. 3 Spot diagram for the panchromatic filter. Spot at the center, corners and edges of the FoV are shown for minimum (600 nm), center (700 nm) and maximum (800 nm) wavelength in filter band.

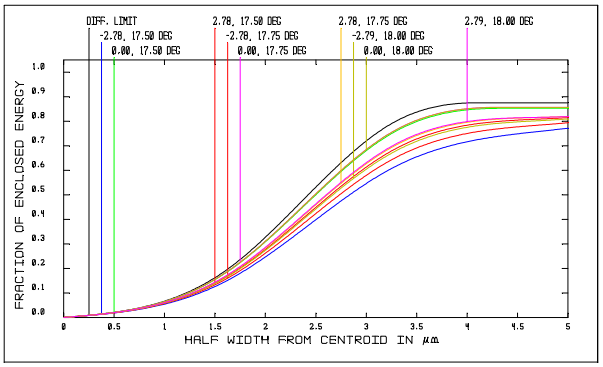

Fig. 4. EE for the panchromatic filter. Different lines correspond to different points in the FoV (center, edges, corners). The values are a mean over the wavelength band of the filter.

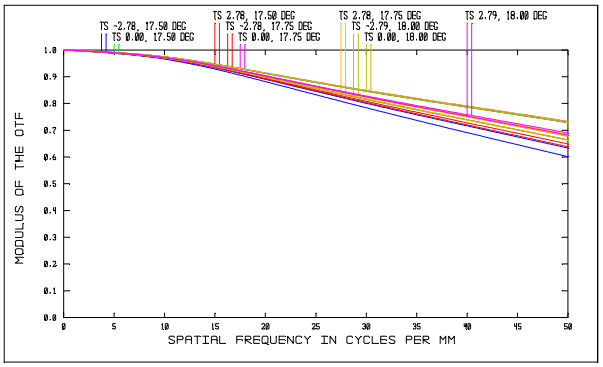

Fig. 5 MTF for the panchromatic filter. Different lines correspond to different points in the FoV (center, edges, corners). The values are a mean over the wavelength band of the filter.

Finally, a preliminary analysis of the camera distortion has been done. Thanks to the adopted Schmidt design and to the position chosen for the AS, the distortion effect is rather limited, being less than 0.3% for all the filter. As an example, the distortion effect for the panchromatic filter is shown in Fig. 6: to clearly see the deformation pattern, the differences between predicted (underlying grid) and real ('×') positions of the chief rays have been multiplied by a factor of twenty; for the considered panchromatic filter FoV, which corresponds to about 8×4 mm^2 on the detector, the distortion is about –0.2%.

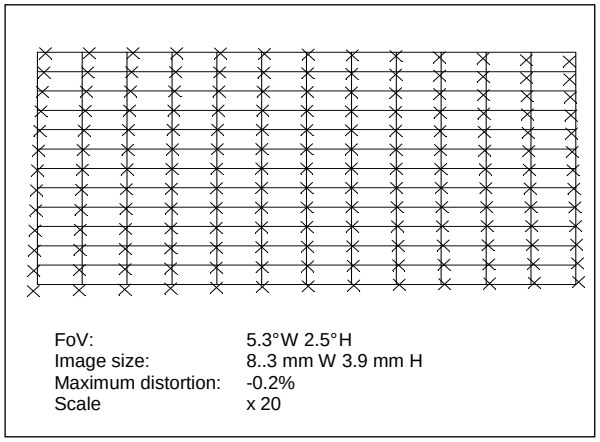

Fig. 6 Grid distortion for the panchromatic filter. Note that real chief ray displacements from theoretical values are multiplied by a factor of twenty to make the distortion effects clearly visible.

2.5 Exposure time

The choice of the exposure time for the images will be derived not only by the intensity of the scene the system will be looking at, but also by the need to prevent the smearing of the image on the pixel due to S/C motion during the acquisition time. The acquisition philosophy is push-frame, or matrix scanner, imaging, in which the composite surface image projected on the detector will be firstly acquired, then buffered and read while the S/C moves; only when the image on the detector has been shifted along track by an amount corresponding to the FoV of each filter, another composite image will be acquired.

Since the S/C velocity at periherm is about 2.2 km/s, this implies that the exposure time has to be less than 5 ms to assure that the image is not smeared, (during 5 ms the surface, imaged on the detector, shifts of about one fifth of a pixel); the repetition time is of the order of 2-5 seconds depending on the position of the S/C during the orbit.

To compute the expected flux and the relative convenient exposure time, a radiometric model which considers the expected properties of the camera (optics and filter transmission and reflectivity properties, detector quantum efficiency) and of the Mercury surface has been implemented. A mean planetary albedo of 0.12 [13] has been considered. For the color filters, an exposure time of 2 ms yields a mean expected flux per pixel of about 4 10^4 photons, with a

signal to noise ratio of 200. For the panchromatic filter, the expected mean flux per pixel, for an exposure time of 0.4 ms, is $9\ 10^4$ photons with a signal to noise ratio of about 300.

2.6 Tolerance analysis

In the analysis of an optical design, the tolerance budgeting is of primary importance. The tolerancing of a stereo camera is a challenging task: in fact not only the desired performance has to be reached and maintained separately for each channel, but also the combination of the two channels and their mutual orientations have to be kept as fixed as possible during all the mission lifetime; in addition, all the optical parameters relative to the DTM reconstruction accuracy have to be fully taken into account. Having in mind these considerations, a preliminary assessment of both manufacturing, alignment and stability tolerance has been undertaken.

The philosophy in tolerancing the system follows directly from the clear subdivision of the system in two part: the fore-optics unit, i.e. the two rhomboid prisms, and the modified Schmidt telescope unit.

Being the prisms positioned into the collimated incoming beam, in principle they are not introducing aberrations or focal variations; they can only be responsible for image shifts. Actually, a rhomboid prism positioned in the object space is insensitive to tilt with respect to three reference axes, and consequently it does not introduce co-registration errors between sub-channels.

For what concerns the prism manufacturing tolerances, it can be mentioned that by means of a suitable manufacturing process (for example the two prisms can be obtained starting from a double prism and cutting it at the middle), the two prisms will have the same angles and consequently possible impacts on sub-channels co-registration can be avoided. However, planarity errors between entrance and exit surfaces have to be controlled to avoid possible increase of aberrations.

Regarding the telescope unit tolerances, the adopted solution with common focusing optics is very performing to avoid, or to limit, co-registration errors and focus differences between the two channels. Possible asymmetries in the actual system can only arise by asymmetries in the realization/mounting of the optical elements. Since optical shop machines usually work spherical surface in symmetric way, the primary reasons for possible asymmetries in the system will be a different realization of the two prisms and/or different relative mounting of the lenses in the correcting doublet or field corrector.

Moreover, any perturbation caused by temperature change or accidental optical element movements have the same repercussions on the two images, in terms of amplitude and direction of the error vector.

The preliminary tolerance analysis results show that the achievable standard manufacturing tolerances of the optical shops for lenses and mirrors, (0.1-0.2% on curvature radius, 1 arcmin on surface parallelism, 10^{-3} on refractive index,..), can be easily compensated. The required compensating motions of the various elements are of the order of ±0.2 mm for decentering and ±0.2° for tilt. The most critical element is the primary spherical mirror, i.e. the only element with optical power in the design, and thus determining the focal length of the full instrument. The primary mirror curvature radius value and its variation clearly propagates into focal length variation of the system.

For the *stability* tolerances, being the optical power of the correcting and field doublet zero, the thermal stability changes can be neglected if the primary mirror and the bench have the same thermal expansion coefficient.

3. CONCLUSIONS

The characteristics and foreseen performance of the Stereoscopic Imaging Channel (STC) for the BepiColombo mission have been presented. The adopted solution, two channels sharing most of the optical elements and the detector, is innovative for a planetary stereo camera, considering that classical stereoscopic designs typically consist of two completely independent twin cameras oriented at the desired stereo angle.

The optical layout is composed by a rhomboid prism, as a fore-optics, one for each sub-channel, followed by a common telescope, which is an off-axis portion of a modified Schmidt design. The telescope is composed by four lenses, two quasi-afocal doublets, plus two mirrors, a focusing and a folding one. All the surfaces of the optical elements are simple spherical or planar surfaces and only the fused silica rad-hard glass has been used.

The aberrations are well compensated all over the camera FoV of about $5° \times 4.5°$ and in the wavelength range between 410 nm and 930 nm, where all the five spectral bands, a panchromatic and four intermediate, are foreseen.

It has been demonstrated that an efficient baffling system is able to well detach the optical paths for stray-light suppression purpose. The designed baffle guarantees that the spurious light level is well controlled and the stray-light signal is negligible in the total noise budget.

Finally, a preliminary tolerance analysis has shown that manufacturing, alignment and stability tolerances are rather relaxed; and the choice of using the rhomboid prism avoid, or reduce, the co-registration error between the two sub-channels. Thus concluding, the global optical performance of the camera assures that it will meet the required scientific constraint.

4. ACKNOWLEDGMENTS

This activity has been realized under the BepiColombo ASI contract to the Istituto Nazionale di Astrofisica (INAF).

5. REFERENCES

1. Davies M. E. et al., *Atlas of Mercury*, NASA SP-423, 1976.
2. Cook A. C. and Robinson M. S., *Mariner 10 stereo image coverage of Mercury*, JGR, Vol. 105 (4), 9429-9443, 2000.
3. Slavin J. A., Owen J. C. J., Connerney J. E. P. and Christon S. P., *Mariner 10 observations of field-aligned currents* at Mercury, Planetary and Space Science, Vol. 45 (1), 133-141, 1997.
4. Hayakawa H., Kasaba Y., Yamakawa H., Ogawa H. and Mukai T., *The BepiColombo/MMO model payload and operation plan*, Advance in Space Research, Vol. 33, 2142-2146, 2004.
5. Thomas N., Spohn T., Barriot J.-P., Benz W., Beutler G., Christensen U., Dehant V., Fallnich C., Giardini D., Groussin O., Gunderson K., Hauber E., Hilchenbach M., Iess L., Lamy P., Lara L.-M., Lognonné P., Lopez-Moreno J. J., Michaelis H., Oberst J., Resendes D., Reynaud J.-L., Rodrigo R., Sasaki S., Seiferlin K., Wieczorek M. and Whitby J., *The BepiColombo Laser Altimeter (BELA): Concept and baseline design*, Planetary and Space Science, Vol. 55(10), 1398-1413, 2007.
6. Flamini E. et al., *SIMBIO-SYS: the Spectrometer and Imagers integrated Observatory SYStem for the BepiColombo Planetary Orbiter*, accepted for publication in Planetary and Space Science, 2008.
7. Da Deppo V., Naletto G., Cremonese G., Debei S. and Flamini E., *A novel optical design for planetary surface stereo-imaging: preliminary design of the Stereoscopic Imaging Channel of SIMBIOSYS for the BepiColombo ESA mission*, Proceedings of the SPIE 6265, 2006.
8. Marra G., Colangeli L., Mazzotta Epifani E., Palumbo P., Debei S., Flamini E. and Naletto G., *The optical design and preliminary optomechanical tolerances of the high resolution imaging channel for the BepiColombo mission to Mercury*, Proceedings of the SPIE 6273, 6273-28, 2006.
9. Capaccioni F., De Sanctis M. C., Piccioni G., Flamini E., Debei S. and SYMBIOSYS International Team, *VIHI: the Visible and Infrared Hyperspectral Imager channel of the SIMBIO-SYS instrument for the BepiColombo mission to Mercury*, AAS/Division for Planetary Sciences Meeting Abstracts, Vol. 37, 2005.
10. Sgavetti M., Pompilio L., Carli C., de Sanctis M. C., Capaccioni F., Cremonese G., Flamini E., *BepiColombo SIMBIO-SYS data: Preliminary evaluation for rock discrimination and recognition in both low and high resolution spectroscopic data in the visible and near infrared spectral intervals*, Planetary and Space Science, 55(11), 1596-1613, 2007.
11. Planche G., Massol C. and Maggiori L., *HRS camera: a development and in-orbit success*, Proceeding of the the 5th International Conference on Space Optics (ICSO 2004), 30 March - 02 April 2004, Toulouse, France, ESA SP-554, 157-164, 2004.
12. Oberst J., Roatsch T., Giese B., Wählisch M., Scholten F., Gwinner K., Matz K.-D., Hauber E., Neukum G., Jaumann R., Ebner H., Spiegel M., vanGasselt S., Albertz J., Gehrke S., Heipke C. and Schmidt R., *The Mapping Performance of The HRSC/SRC In Mars Orbit*, XXth ISPRS Congress, 12-23 July 2004 Istanbul, Turkey, Commission 4, 1318-1323, 2004.
13. Warell J., Properties of the Hermean regolith: IV. *Photometric parameters of Mercury and the Moon contrasted with Hapke modelling*, Icarus, Vol. 167, 271-286, 2004.